JCTC Journal of Chemical Theory and Computation

A Subsystem TDDFT Approach for Solvent Screening Effects on Excitation Energy Transfer Couplings

Johannes Neugebauer,*,† Carles Curutchet,‡,§ Aurora Muñoz-Losa,|| and Benedetta Mennucci||

Gorlaeus Laboratories, Leiden Institute of Chemistry, Leiden University, P.O. Box 9502, 2300 RA Leiden, The Netherlands, Department of Chemistry, 80 St. George Street, Institute for Optical Sciences and Centre for Quantum Information and Quantum Control, University of Toronto, Toronto, Ontario M5S 3H6 Canada, Institut de Química Computacional and Departament de Química, Universitat de Girona, Campus Montilivi 17071 Girona, Catalonia, Spain, and Dipartimento di Chimica e Chimica Industriale, Università di Pisa, via Risorgimento 35, 56126 Pisa, Italy

Received March 16, 2010

Abstract: We present a QM/QM approach for the calculation of solvent screening effects on excitation-energy transfer (EET) couplings. The method employs a subsystem time-dependent density-functional theory formalism [*J. Chem. Phys.* **2007**, *126*, 134116] and explicitly includes solvent excited states to account for the environmental response. It is investigated how the efficiency of these calculations can be enhanced in order to treat systems with very large solvation shells while fully including the environmental response. In particular, we introduce a criterion to select solvent excited states according to their approximate contribution weight to the environmental polarization. As a model system, we investigate the perylene diimide dimer in a water cluster in comparison to a recent polarizable QM/MM method for EET couplings in the condensed phase [*J. Chem. Theory Comput.* **2009**, *5*, 1838]. A good overall agreement in the description of the solvent screening is found. Deviations can be observed for the effect of the closest water molecules, whereas the screening introduced by outer solvation shells is very similar in both methods. Our results can thus be helpful to determine at which distance from a chromophore environmental response effects may safely be approximated by classical models.

1. Introduction

One of the fundamental steps in the primary events of photosynthesis is the transfer of excitation energy from a light-absorbing unit to a photosynthetic reaction center.[1] In the simplest case, this excitation-energy transfer (EET), which is a nonradiative process, involves the de-excitation of one chromophore (donor) together with the excitation of another pigment (acceptor).[2] The main mechanism for this transfer is a Coulomb interaction between the transition densities of the two electronic transitions on the donor and acceptor, which for long distances can be described in terms of a transition-dipole interaction (Förster dipole coupling).[3,4] Other mechanisms can play a role in short separations of the donor and acceptor if there is considerable overlap of the monomer wave functions.[5,6] EET is an important effect not only in natural photosynthesis but also in artificial photosynthetic systems and optoelectronic devices.

While EET is a dynamic phenomenon, one of the essential ingredients in calculations of EET rate constants is the electronic coupling between the donor and acceptor transition, which is related to the energy difference between the coupled stationary electronic states ("excitonic states") of the two chromophores. Consequently, much effort has been spent on the accurate calculation of transition densities of

* Corresponding author e-mail: j.neugebauer@chem.leidenuniv.nl.

† Leiden University.

‡ University of Toronto.

§ Universitat de Girona.

|| Università di Pisa.

10.1021/ct100138k © 2010 American Chemical Society
Published on Web 05/19/2010

pigment molecules involved in EET and their electronic couplings ("excitonic couplings") during the past 10 to 15 years.[7–22] One of the open problems for a realistic description of excitation energy transfer rates is the inclusion of solvent effects, which is often just estimated on the basis of the dielectric constant of the environment. The screening of the Coulomb coupling by the solvent (or a general environment) can lead to considerable variations in the EET rates, especially for couplings at short and medium ranges.[11,14,23–27]

Recent investigations have addressed the possibilities of describing solvent screening effects on EET including more and more details of the environment. The approach presented in ref 14 is based on the polarizable continuum model (PCM)[28] and is able to consider the influence of the shape of the pigment molecules on the EET screening by the solvent. In contrast to this, the simple Förster approximation for the screening factor of EET rates considers a screening of point dipoles embedded in a dielectric continuum, which leads to problems at short range.

In ref 27, a polarizable QM/MM approach in combination with an ensemble averaging was developed for the simulation of solvent screening effects. It could be shown that, for homogeneous media, QM/MM and PCM results for the environmental screening are very similar. However, for heterogeneous media as present in proteins, QM/MM methods are expected to be more reliable, since they can model the environment in atomistic detail. While this is a clear advantage of the polarizable QM/MM approach, it requires a careful parametrization of the MM part. Furthermore, at very short range, the representation of the electrostatic effect of the environment in terms of point charges and induced dipoles as used in many QM/MM approaches may limit the overall accuracy of the calculation (cf. the benchmark study on protein effects on electronic spectra in ref 29). For certain specific effects, it may be necessary to include the relevant parts of the environment in the QM part of the calculation; examples addressing effects of hydrogen bonding, axial ligation, and effects of nearby charged residues on the absorption bands of bacteriochlorophyll molecules in a photosynthetic light-harvesting complex are given in refs 17 and 30. It should be noted that a direct assessment of such specific effects on the basis of experimental data is rather involved; for an example, see ref 31.

QM/MM approaches can be tested by comparing them to fully quantum chemical approaches. The study in ref 27 employed supermolecular quantum chemical calculations for this purpose, in which both interacting chromophores and the surrounding solvent were treated with configuration interaction singles (CIS). A very good agreement for both types of calculations was reported. However, supermolecular reference calculations are very demanding in terms of computer time and pose additional complications. In particular, for nonhybrid density functionals, many artificially low-lying charge-transfer excitations occur for solvated systems[32] due to the incorrect description of charge-transfer excitations when using exchange-correlation kernels obtained within the adiabatic local density approximation (ALDA) or the adiabatic generalized gradient approximation (AGGA).[33–40] This further increases the computational effort and hampers the identification of the excitonic states, which is a prerequisite for extracting excitonic coupling constants from supermolecular calculations.

An alternative for the calculation of excitonic couplings from a purely quantum chemical approach is provided by subsystem methods within density functional theory. A subsystem formulation of density functional theory (DFT) was developed by Cortona in 1991[41] in the context of atomic subsystems in crystals (see also the earlier work by Senatore and Subbaswamy[42]). Subsequently, Wesolowski and Warshel proposed the so-called frozen-density embedding (FDE) method,[43] which can be regarded as a simplified and efficient subsystem method, in which only the electron density of an active part is optimized. The freeze-and-thaw method presented in ref 44 allows for a continuous transition between both extremes (fully frozen or fully relaxed environment) in the case of a partitioning into two subsystems, the active part and an environment. A fully relaxed subsystem DFT treatment involving many molecular subsystems was presented in ref 45, and a general setup allowing for different relaxation strategies of different subsystems is available[46] in the Amsterdam Density Functional program.[47,48]

An extension of the FDE method to excited states in terms of time-dependent DFT (TDDFT) was presented by Casida and Wesolowski.[49] On the basis of this work, a generalized subsystem TDDFT or coupled FDE-TDDFT (FDEc) approach was formulated by one of the present authors in refs 50 and 51, and efficient algorithms for calculating excitonic couplings for large aggregates of pigments were developed.[17,50] While the initial studies considered environmental effects only in terms of an effective embedding potential,[17,50] first applications that include solvent screening effects on exciton splittings of small models were presented in ref 52.

Here, we are going to investigate solvent screening effects in subsystem TDDFT in more detail and discuss possible strategies for the efficient solution of the computational problems involved. As a test system, we employ the intense low-lying $\pi \rightarrow \pi^*$ transition of the solvated perylene diimide (PDI) dimer, which was investigated in ref 27.

2. Theory

The FDEc approach presented in refs 17 and 50 allows calculations of the excitation energies of a system composed of several molecules in two steps. First, the uncoupled FDE (FDEu) excitation energies are calculated; i.e., local excitations of all constituent molecules are obtained, embedded in an environment formed by all other molecules. These calculations employ the ground-state FDE embedding formalism as proposed by Wesolowski and Warshel,[43] in which the environmental density is obtained as a sum of all other molecules' densities. To obtain optimum subsystem densities, we iteratively apply freeze-and-thaw cycles[44] to all subsystems, so that effectively a variational subsystem density functional theory treatment is performed.[41,45,53] Local excited states are then obtained for all subsystems with the approximate form[54] of the FDE generalization to excited states[49] that restricts the response to the active subsystem only. In a second step, delocalized excited states of the entire

aggregate are calculated by coupling these local excitations following the subsystem TDDFT formalism presented in ref 17.

The main question that arises in approximate applications of the subsystem TDDFT formalism is the selection of states to be coupled. A direct connection to exciton coupling models can be made if only the relevant local excited states of the chromophores are coupled. These states will be called "reference states" in the following. In the present work, this would correspond to the intense low-lying $\pi \rightarrow \pi^*$ excitation of the perylene diimide molecules. In ref 50, it was tested how the inclusion of additional excited states of the pigment molecules influences both the vertical excitation energies of the full system and the excitonic splitting between the reference states. A typical criterion that was used in the original implementation to determine states that have to be included[50] was the energy difference between a particular excited state and the reference states, since high-lying excited states only have a minor effect on the excitonic states. When modeling solvent effects, however, the situation is somewhat more complicated. The solvent screening can, in a linear-response TDDFT framework, be understood as a cumulative effect caused by many excited states of the solvent system. Consequently, a very large number of excited states would have to be included, which considerably increases the effort for FDEc calculations.

In order to achieve a reasonable representation of the solvent response, we have adopted the following strategy: We first determine how many excited states are necessary to represent the (isotropic) polarizability of a solvent molecule to a good accuracy in terms of the sum-over-states (SOS) expression (Hartree atomic units are used throughout)

$$\alpha(\omega) = \frac{2}{3}\sum_{\nu}\frac{\omega_\nu}{\omega_\nu^2 - \omega^2}|\mu_{0\nu}|^2 \qquad (1)$$

where the sum runs over all excited states ν with excitation energies ω_ν and transition dipole moments $\mu_{0\nu}$ of the solvent molecule. Once these excitations are calculated for all (embedded) solvent molecules, they are sorted according to their contribution to the SOS polarizability expression in descending order. From this list of states, we choose the first k states, where the number k is determined in such a way that the cumulative contribution of these states is larger than a preselected threshold percentage p of the full SOS polarizability (obtained when including all precalculated excited states). Figure 1 shows the results for a water molecule (PBE/TZP) in the static limit. In this calculation, all singlet−singlet excitations within the TZP basis set have been calculated (130 in total). The dashed curve shows the cumulative polarizability contribution for the excited states when ordered by energy. This is a straightforward choice, since excited states are usually calculated with Davidson-type subspace iteration methods, which yield the lowest-energy transitions.[55,56] The solid line shows the results obtained if the excited states are ordered by their contribution to α. About 90 states are needed to arrive at the converged isotropic polarizability value when the states are ordered by energy, whereas a similar convergence is already reached

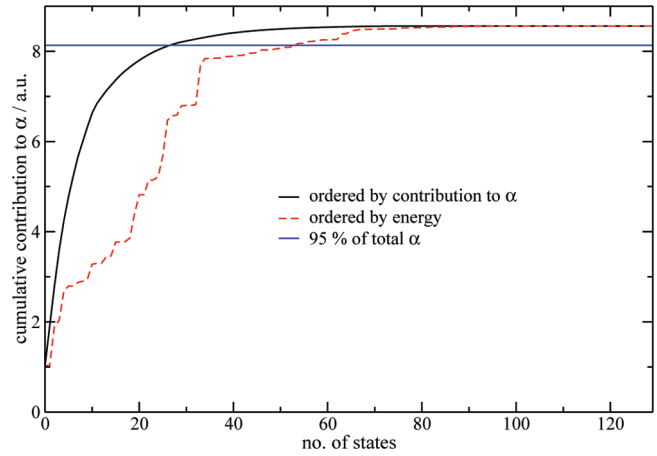

Figure 1. Cumulative contribution to the isotropic SOS polarizability of water (PBE/TZP, optimized structure, static limit) as a function of the number of excited states. Shown are results for contributions ordered according to the energy of the excited state (dashed line) and according to the contribution to the polarizability (solid line). The horizontal line represents a 95% threshold to the total polarizability.

with 60 states if the states are sorted by increasing contribution to α. The horizontal line in Figure 1 indicates a 95% threshold of the polarizability. As will be shown below, this is typically sufficient for the calculation of screening effects on excitonic couplings. It can be seen that this threshold is reached with 53 states in the energy-sorted curve, whereas only 27 states are needed from the list ordered by polarizability contributions. This shows that a fairly small number of excited states may be sufficient to reproduce the polarizability of a water molecule. Nevertheless, the total number of coupled states increases tremendously when considering the solvent response. Another approximation that can be introduced is thus that solvent excited states are only coupled to the dye molecules' excited states, whereas intersolvent couplings are neglected. This approximation will be tested in section 4.

As discussed in refs 17 and 52, the elements of the matrix $\tilde{\mathbf{\Omega}}$, which describe the couplings between transitions on different subsystems, are calculated as

$$\tilde{\Omega}_{\mu_A\nu_B} = \int d\mathbf{r}_1 \sum_{(ia)_A} 2F_{(ia)_A\mu_A}\sqrt{\omega_{(ai)_A}}\phi_{i_A}(\mathbf{r}_1)\delta v^{\mathrm{ind}}_{A,\nu_B}(\mathbf{r}_1)\phi_{a_A}(\mathbf{r}_1) \qquad (2)$$

Here, $F_{(ia)_A\mu_A}$ is the solution factor describing the local excitation μ_A in subsystem A, ϕ_{i_A} and ϕ_{a_A} are occupied and virtual, respectively, orbitals in subsystem A, and $\omega_{(ai)_A}$ is their orbital energy difference; $\delta v^{\mathrm{ind}}_{A,\nu_B}$ is the potential that is induced in system A by the local electronic transition ν_B of system B. The transition density of transition ν_B enters the induced potential, while the sum over the orbital products $F_{(ia)_A\mu_A}(\omega_{(ai)_A})^{1/2}\phi_{i_A}\phi_{a_A}$ can be identified with the transition density of transition μ_A. In principle, $\tilde{\mathbf{\Omega}}_{\mu_A\nu_B}$ should be symmetric, since only local response kernels are employed to calculate $\delta v^{\mathrm{ind}}_{A,\nu_B}$. In practice, however, two different kinds of approximations are introduced that can make $\tilde{\mathbf{\Omega}}$ nonsymmetric: The induced potential is constructed on the basis of a *fitted* transition density,[50,57] and the integration in eq 2 is performed in ADF by *numerical* integration.

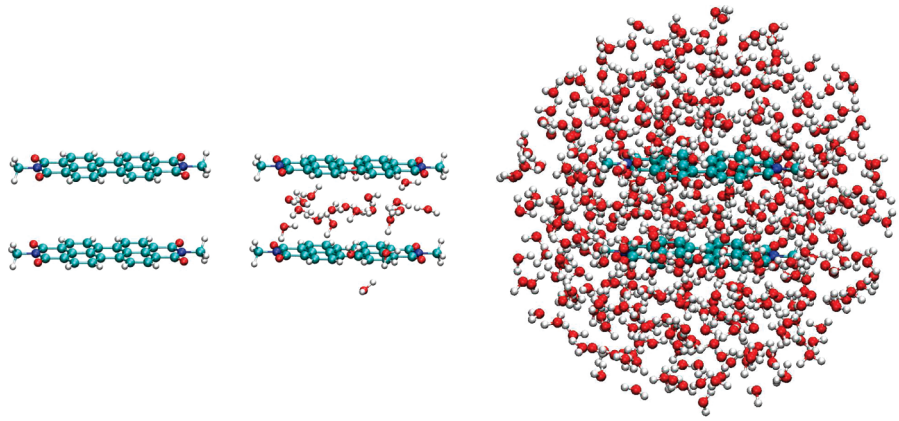

Figure 2. Structure of the (solvated) PDI dimer from ref 27. Left, isolated dimer; middle, 7 Å solvation shell; right, 15 Å solvation shell.

The strategy introduced in refs 17 and 50 was to consider one of the subsystems (A) as the "active" subsystem and to evaluate its transition density exactly (but numerically). The other system is treated as the environmental system (B), and its transition density is fitted. In the current study, it is computationally advantageous to perform the numerical integration step for the smaller subsystems, i.e., the solvent molecules. We will refer to this as a "transpose construction" of $\tilde{\mathbf{\Omega}}$.

In the FDEc calculations involving solvent response, no direct solvent contribution to the coupling can be calculated. The reason is that in the FDEc treatment the solvent response explicitly appears in the TDDFT eigenvalue problem in terms of solvent excited states, whereas it is contained implicitly in the interchromophore couplings in the QM/MMpol scheme and the PCM model. In order to extract excitonic coupling constants V from the FDEc calculations under the influence of the solvent response, we therefore use the expression derived from a secular determinant for Frenkel excitons of two-level chromophores,[10] as has been used in ref 27 to extract coupling constants from supermolecular calculations:

$$V = \frac{1}{2}\sqrt{(\omega_+ - \omega_-)^2 - (\omega_D - \omega_A)^2} \qquad (3)$$

where $\omega_{D,A}$ are the local excitation energies of the donor and acceptor, respectively, and $\omega_{+,-}$ are the energies of the upper and lower, respectively, excitonic state.

3. Computational Details

All subsystem (TD)DFT calculations have been performed with a modified version[17,50] of the ADF 2008 program.[47,48] Supermolecular reference calculations and calculations on isolated molecules were carried out with the RESPONSE module of ADF.[57] We use the Perdew−Burke−Ernzerhof (PBE) exchange-correlation functional; for the LDA part, the Perdew−Wang (PW92) parametrization was employed, which corresponds to the default in the ADF 2009 version but is at variance with the ADF 2008 defaults. The TZP basis set from the ADF basis set library has been used for all ADF calculations. For the nonadditive kinetic energy contribution in subsystem DFT calculations, the so-called GGA97 generalized-gradient approximation (GGA) to the kinetic-energy functional was employed.[58] It has the same functional form for the enhancement factor $F(s)$ as the exchange functional of Perdew and Wang[59] and is therefore often denoted as PW91k. It was parametrized for the kinetic energy by Lembarki and Chermette.[60] For all (subsystem) TDDFT calculations, we applied the adiabatic local density approximation for the exchange-correlation kernel. In the case of subsystem TDDFT, also the kinetic-energy component of the kernel is approximated by the local-density (Thomas-Fermi) approximation.

QM/MM calculations with a polarizable force-field, denoted as QM/MMpol in the following, have been performed as described in ref 27 with a locally modified version of the Gaussian 03 package.[61] All QM/MMpol calculations employed the PBE exchange-correlation functional and a cc-pVTZ basis set.[62] The parametrization of the force-field part was adopted from ref 27 and consists of a set of distributed atomic polarizabilities calculated using the LoProp approach[63] combined with ESP charges fitted to the electrostatic potential, both obtained at the B3LYP/aug-cc-pVTZ level.

Test calculations on a PDI monomer resulted in excitation energies of 2.134 (PBE/TZP) and 2.145 eV (PBE/cc-pVTZ). The corresponding oscillator strengths are 0.548 (PBE/TZP) and 0.542 (PBE/cc-pVTZ). Excitonic splitting energies for the low-lying $\pi \rightarrow \pi^*$ transitions based on supermolecular calculations were obtained as 0.0914 eV (PBE/TZP) and 0.0900 eV (PBE/cc-pVTZ). This shows that the results from the calculations with Slater-(TZP) and Gaussian-type (cc-pVTZ) basis sets are in very good agreement.

Graphics of the molecular structures were generated with the program VMD.[64]

4. Coupled Response of Solvated Dimers

The structure of the perylene diimide dimer investigated here is shown in Figure 2. It is the same structure investigated in ref 27 (intermolecular distance: 7 Å). Solvation shells with radii between 7 and 11 Å around the center of the pigment dimer have been considered in the initial tests to investigate the screening effect, while for the comparison with the QM/MMpol approach, extended solvation shells with up to 15 Å cutoffs (>1400 atoms in total) have been employed.

Table 1. Excitation Energy (E_u, in units of eV) and Oscillator Strength f_u of the Upper Excitonic State and Excitonic Splitting ΔE (in units of cm^{-1}) for the Isolated PDI Dimer with a Distance of 7 Å

	E_u	ΔE	f_u
iso, uncoupled	2.134	0	0.548
FDEu	2.133	0	0.550
FDEc	2.178	734	1.100
super, iso	2.174	737	0.956

Table 2. Excitation Energy (E_u, in units of eV) and Oscillator Strength f_u of the Upper Excitonic State and Excitonic Splitting ΔE (in units of cm^{-1}) for the PDI Dimer for a 7 Å Solvation Shell with Different Thresholds p for the Cumulative Polarizability Contribution[a]

p	# states	E_u	ΔE	f_u
FDEu		2.118	11	0.543
0.000	20	2.161	725	1.079
0.100	42	2.160	735	1.071
0.200	63	2.159	744	1.063
0.300	89	2.157	734	1.048
0.400	117	2.155	728	1.032
0.500	146	2.154	725	1.021
0.600	179	2.152	718	1.009
0.700	226	2.150	710	0.997
0.800	294	2.149	707	0.984
0.900	461	2.147	704	0.971
0.950	654	2.145	702	0.964
0.990	1097	2.144	699	0.959
0.999	1561	2.144	698	0.957
all	2120	2.144	697	0.957
super		2.115	644	0.768

[a] Also shown is the number of states that have to be coupled. FDEu denotes the uncoupled calculation; in the case of $p = 0.000$, only the 20 excited states calculated for the PDI molecules are coupled.

As a first test of the subsystem methodology to describe EET couplings, we calculated the excitation energies of the PDI dimer without the water environment in a supermolecular and a subsystem TDDFT calculation. The results are compared in Table 1. The FDEu data hardly differ from those of the isolated monomer calculations, as expected, because of the rather large distance of 7 Å between the monomers. The FDEc calculations lead to the expected splitting and reproduce the splitting energy of the supermolecular calculation very well (734 compared to 737 cm^{-1}). Also, the energy of the intense upper excitonic state from FDEc agrees nicely with the supermolecular results; the oscillator strength is, however, somewhat overestimated. A possible reason could be a basis set superposition effect in the supermolecular calculation (cf. the discussion of such effects in ref 51).

We now consider the smallest solvated system (7 Å solvation shell) to test the necessary approximations for the inclusion of the solvent response. In all calculations, 10 excited states per PDI molecule are included. Table 2 contains the results for different thresholds (percentages of the total SOS polarizability) for the cumulative polarizability contribution. The resulting splitting energies are also shown in Figure 3. The uncoupled FDE calculation leads to a small splitting between the two monomer transitions due to slightly different local environments in this snapshot. If the coupling between the PDI monomers is included in the calculation,

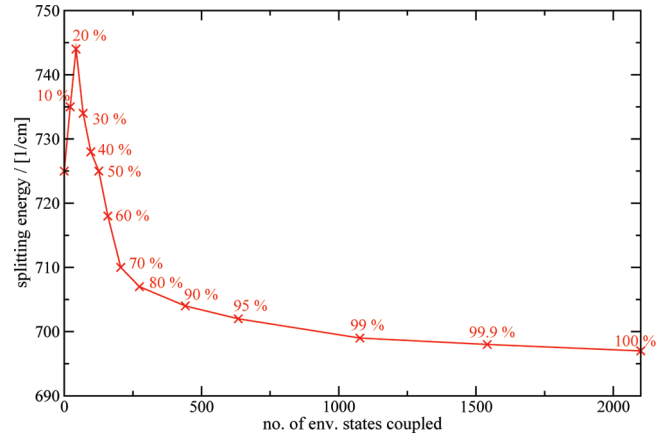

Figure 3. Splitting energies between the two excitonic states in the PDI dimer with a 7 Å solvation shell as a function of the threshold p for the cumulative polarizability contribution of the coupled states.

but no solvent response is taken into account, a splitting of 725 cm^{-1} is observed. Including more and more environmental states first increases the energy gap to 744 cm^{-1} if 20% of the polarizability is reproduced and then decreases it to a final value of 697 cm^{-1} if all environmental states are included. If 95% of the polarizability is reproduced by the coupled states, the splitting energy is converged within 5 cm^{-1} (0.7%). This threshold will be used in all subsequent calculations.

A supermolecular calculation on this system resulted in a somewhat smaller splitting energy of 644 cm^{-1}. This discrepancy is not very large on an absolute scale. But there is a more pronounced difference in the results from FDEc and from the supermolecular calculation for the *change* in the splitting energy from the isolated PDI dimer to the solvated system studied here: In the FDEc case, the splitting reduces from 734 to 697 cm^{-1}, whereas in the supermolecular case, it decreases from 737 to 644 cm^{-1}. It should be noted, however, that the identification of the lower excitonic state in the supermolecular calculation is not entirely unambiguous. Many additional excited states appear, several of which are of the intermolecular charge-transfer type and thus significantly underestimated in our calculations (see the related problem in ref 32). Such difficulties do not appear in the absence of solvent molecules. Although an assignment can be made on the basis of the dominant orbital transitions, these orbital transitions also mix with other excitations for the PDI dimer, which are slightly lower in energy and would thus increase the splitting energy in the solvated case. Other reasons could be the monomer basis sets used to expand the (response) densities of the subsystems in the FDEc calculations. These basis sets are thus the same in the solvated and nonsolvated case, whereas the excitonic states in the supermolecular calculation benefit from the presence of basis functions at the solvent molecules. Also, the different accuracy of the available approximations for the kinetic-energy potential and kernel for different interaction strengths could play a role. These approximations will work better the smaller the subsystem density overlap is.[65,66] The PDI monomers in the isolated dimer are well separated, but water molecules appear quite close to the dye molecules

Table 3. Excitonic Coupling Constants (in units of cm^{-1}) for the PDI Dimer for Different Sizes of the Solvation Shell (cutoffs in units of Å)[a]

cutoff	nsc	nisc	$p = 0.95$	$p = 0.95$, transp	full	QM/MMpol
7	363	359	351	353	348	371
8	362	345	335	337	332	360
9	366	335	328	328	322	359
10	363	319	315	315	310	349
11	365	307	306	306		341

[a] nsc, no solvent couplings; nisc, no inter-solvent couplings; p refers to the cumulative polarizability threshold; full, all solvent couplings fully included. The label "transp" refers to the transpose construction of $\tilde{\Omega}$.

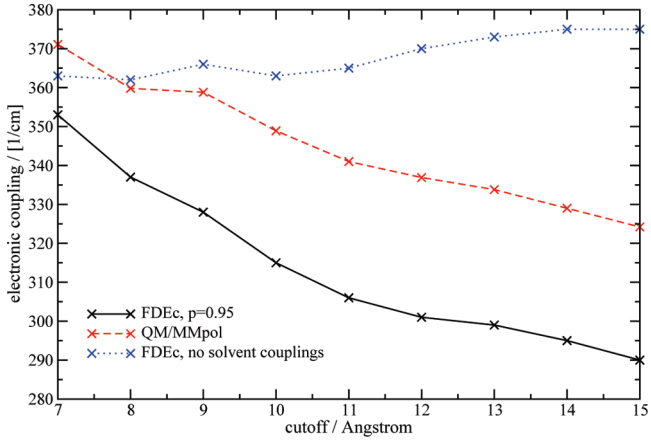

Figure 4. Excitonic coupling constants for the PDI dimer with increasing solvation shell cutoffs. Results are shown for FDEc calculations neglecting any solvent couplings or employing a cumulative polarizability threshold of $p = 0.95$ as well as for QM/MMpol calculations.

in the solvated dimer, so that the accuracy of the kinetic-energy contributions may be slightly worse in the solvated case.

As a next step, we investigate the dependence of the excitonic splitting on the size of the solvation shell. Table 3 contains the coupling constants calculated according to eq 3 for several different approximations. The column labeled "nsc" refers to calculations with "no solvent couplings"; i.e., the response of the environment is neglected. Only the environmental effect on the ground-state properties is taken into account in terms of the FDE potential (apart from a small modification of the exchange-correlation kernel, see ref 52 for details). As can be seen, there are only small effects on the calculated coupling constants (<5 cm^{-1} compared to the coupling of 367 cm^{-1} found for the isolated PDI dimer), which means that there is hardly any effect of the environmental potential on the transition densities of the monomers. The additional data for cutoffs of 12 to 15 Å presented in Figure 4 indicate a slight increase, so that the coupling converges to 375 cm^{-1}, still within 8 cm^{-1} of the isolated dimer. In contrast to that, all other calculations predict a decrease in the coupling constants with increasing cutoff for the solvation shell. If only solute−solvent couplings are included in addition to the solute−solute couplings, V decreases by 52 cm^{-1} from 359 cm^{-1} (7 Å) to 307 cm^{-1} (11 Å). If a cumulative polarizability threshold of $p = 0.95$ is applied, V decreases by 45 cm^{-1} from 351 cm^{-1} to 306 cm^{-1}. This shows that the neglect of intersolvent couplings leads to the same qualitative behavior, although the deviation is larger for smaller solvation shells. As a reference, we also carried out fully coupled calculations, in which all solvent couplings are included. These calculations are still quite demanding and have therefore only been carried out for cutoffs up to 10 Å. The results show the same trend as the $p = 0.95$ values but are systematically shifted by about 3 to 6 cm^{-1}.

Table 3 also shows the results obtained with a transpose construction of $\tilde{\mathbf{\Omega}}$ as defined in section 2. It can be seen that the deviation between the two different construction schemes is very small (0 to 2 cm^{-1}). Since the transpose construction is a great computational advantage for the system studied here, it was employed for the calculations presented in the following.

A comparison of the EET couplings calculated with FDEc ($p = 0.95$) and the corresponding values obtained from the QM/MMpol calculations is presented in Figure 4. For cutoffs of 10 Å or larger, the splittings calculated with FDEc and QM/MMpol run more or less parallel, with an offset of about 35 cm^{-1}. For smaller cutoffs of the solvation shell, however, the difference between the two curves decreases to 18 cm^{-1} (cutoff of 7 Å), and the two curves are not parallel anymore. In other words, the effect of outer solvation shells is described in the same way in FDEc and QM/MMpol calculations, whereas there is a slight quantitative disagreement for the nearest solvent molecules.

Interestingly, the QM/MMpol slight overestimation of the FDEc couplings is similar to that found in ref 27, where QM/MMpol was compared to full quantum chemical calculations. Also in this work, supermolecular calculations indicate smaller splittings. These findings suggest that short-range nonelectrostatic interactions between the dyes and the first solvation shell, neglected in the QM/MMpol scheme, seem to slightly attenuate the electronic coupling.

5. Solvent Screening Factors

In the QM/MMpol approach presented in ref 27, the EET couplings V are obtained as a sum of two terms:

$$V = V_s + V_{\text{explicit}} \tag{4}$$

where V_s is the Coulomb plus exchange-correlation interaction of the transition densities $\rho^T_{D,A}$ of the *solvated* donor (D) and acceptor (A) systems:

$$V_s = \int d\mathbf{r} \int d\mathbf{r}'\, \rho^T_A(\mathbf{r}')\left(\frac{1}{|\mathbf{r}-\mathbf{r}'|} + f_{xc}(\mathbf{r},\mathbf{r}')\right)\rho^T_D(\mathbf{r}) - \omega_0 \int d\mathbf{r}\, \rho^T_A(\mathbf{r})\, \rho^T_D(\mathbf{r}) \tag{5}$$

The last term is an overlap contribution that arises because the interaction in ref 27 is treated as a perturbation of separated systems A and D; it is usually very small.[14] In the present study, it never contributes more than 0.6 cm^{-1} to the total coupling. The explicit solvent contribution V_{explicit} describes the interaction of systems A and D that is mediated by the environment. To be more precise, it is calculated as

Table 4. Excitonic Coupling Constants V_s (from QM/MMpol; in units of cm^{-1}) for the PDI Dimer and Solvent Screening Factors $s_{QM/MMpol}$ and s_{FDEc} as a Function of the Cutoff Distance for the Solvent Shell[a]

cutoff	V_s	$s_{QM/MMpol}$	s_{FDEc}
7	391	0.95	0.90
8	406	0.89	0.83
9	432	0.83	0.76
10	437	0.80	0.72
11	446	0.76	0.69
12	458	0.73	0.66
13	465	0.72	0.64
14	470	0.70	0.63
15	472	0.69	0.61

[a] Note that the same V_s values have been employed for both sets of solvent screening factors, since V_s is not directly available from FDEc calculations.

the Coulomb interaction of the transition density ρ_A^T with the dipoles induced in the environment by ρ_D^T,[27]

$$V_{\text{explicit}} = -\sum_k \left(\int d\mathbf{r}\, \rho_A^T(\mathbf{r}) \frac{(\mathbf{r}_k - \mathbf{r})}{|\mathbf{r}_k - \mathbf{r}|^3} \right) \mu_k^{\text{ind}}(\rho_D^T) \qquad (6)$$

The induced dipoles μ_k^{ind} at positions $\mathbf{r}_k$ are employed in the QM/MMpol model to simulate the polarization of the environment.

Solvent screening factors s can then be calculated as[27]

$$s = \frac{V}{V_s} = \frac{V_s + V_{\text{explicit}}}{V_s} \qquad (7)$$

The main difference with respect to the FDEc approach is that the transition densities employed in the calculation of V_s, eq 5, are obtained for the solvated monomers *including* an environmental response contribution. The explicit contribution to the coupling thus reflects the differential solvent polarization when the interaction between the monomers is "switched on".

In contrast to that, the FDEc couplings are calculated on the basis of local transition densities of the subsystems that neglect the environmental response contribution, and the *entire* solvent response enters the calculation of the total EET couplings. If we would calculate the solvent screening factor as the ratio between the FDEc results without solvent couplings and the fully coupled FDEc data, we would thus employ a different definition of the solvent screening factor (see below).

If we assume the V_s values from the QM/MMpol calculations, which we cannot directly access on the basis of the FDEc approach, and combine them with the total couplings V calculated from FDEc, we can determine the solvent screening factors. This is done in Table 4. The values obtained with the polarizability criterion $p = 0.95$ have been employed for that purpose. Also shown are the QM/MMpol V_s values as well as the QM/MMpol solvent screening factors. In both cases, the solvent screening decreases, and the FDEc solvent screening factor is systematically lower than the QM/MMpol result, as could be expected from the coupling constants. Nevertheless, there is a fair agreement between the two sets of calculations, and the trend is clearly the same.

Table 5. Solvent Screening Factors $\tilde{s}$ Calculated as the Ratio of the Excitonic Coupling in the Solvent Shell and the Coupling in a Vacuum for the PDI Dimer as a Function of the Cutoff Distance for the Solvent Shell

cutoff	$\tilde{s}_{QM/MMpol}$	$\tilde{s}_{FDEc}$
7	1.02	0.96
8	0.99	0.92
9	0.99	0.89
10	0.96	0.86
11	0.94	0.83
12	0.93	0.82
13	0.92	0.81
14	0.91	0.80
15	0.89	0.79

The above definition of the screening factor is consistent with the factor assumed in Förster theory, which scales a dipole−dipole interaction obtained from transition dipole moments measured for the noninteracting dyes in solution.[67] However, an alternative definition of the screening factor that accounts for the entire solvent effect, and thus allows a more in-depth comparison between the FDEc and QM/MMpol methods, is given by the ratio

$$\tilde{s} = \frac{V_{\text{solution}}}{V_{\text{vacuum}}} \qquad (8)$$

of the coupling constant of the solvated dimer, V_{solution}, divided by the coupling constant of the dimer in a vacuum, V_{vacuum} (367 cm^{-1} for FDEc and 363 cm^{-1} for QM/MMpol). Table 5 reports the results adopting this alternative solvent screening factor $\tilde{s}$. Interestingly, the coupling constant for a 7 Å cutoff with the QM/MMpol method is larger in solution than in the isolated dimer. The solvent screening factor $\tilde{s}_{QM/MMpol}$ decreases by 12.6% from 1.02 (7 Å) to 0.89 (15 Å). The FDEc solvent screening factor $\tilde{s}_{FDEc}$ shows a somewhat stronger decrease of 17.9% from 0.96 to 0.79. Both sets of screening factors are considerably larger than those obtained with the original definition shown in Table 4.

6. Conclusion

In this work, we have demonstrated that it is possible to include solvent screening effects into the calculation of excitonic splittings and EET couplings in the subsystem TDDFT formalism. Although the computational effort is considerably increased compared to calculations for isolated chromophores, several developments and approximations have been presented that allow an enhancement of the efficiency of the calculations. In particular, the number of solvent excited states needed to reproduce the environmental response effect could considerably be reduced by employing a polarizability-related criterion to select the coupled states. Furthermore, a transpose construction of the coupling matrix, in which the numerical integration step of the matrix elements is always carried out for the smaller subsystem, greatly reduces the computer time necessary for the calculation. Both procedures do not affect the magnitude of the calculated coupling constants significantly, and deviations were always within 6 cm^{-1} or 0.7 meV. This shows that the full response of environmental systems with more than 1000 atoms can

be treated accurately and fully quantum mechanically with the present approach. The results for the transpose construction also underline that the approximation of a symmetric coupling matrix made in ref 50 is well justified. Additional approximations can involve the neglect of intersolvent couplings, although this leads to slightly larger deviations from the fully coupled results.

FDEc and QM/MMpol agree rather well on the EET couplings of the solvated systems, and on their dependence on the size of the solvation shell. Discrepancies between the two approaches are on the order of 20 to 35 cm^{-1} (6 to 10%). In particular, the effect of outer solvent molecules is very similar in both methods, whereas the deviations are a bit larger for smaller solvation shells.

Since FDEc and QM/MMpol describe the solvent response effects in different ways, it is not straightforward to calculate screening constants for FDEc in the way defined in ref 27. However, if the unscreened EET couplings are taken from the QM/MMpol calculation, then FDEc leads to a similar screening dependence on the cutoff radius of the solvation shell as QM/MMpol, although the predicted FDEc screening constants are somewhat smaller. This also holds for an alternative definition of the solvent screening as the ratio between the EET couplings in solution and in a vacuum, which in general leads to larger solvent screening constants.

This study thus indicates that there are small differences in the description of short-range electronic couplings between the subsystem TDDFT (FDEc) approach and the polarizable QM/MM approach. It also allows an estimation of the size of the solvation shell in which these differences become negligible. In the present example, it turned out that solvent molecules beyond the 10 Å cutoff have roughly the same effect in both approaches. Our work thus forms the basis for multiscale approaches to model the screening effect of general environmental systems on EET couplings that include the possibility to control the error introduced by different representations of different parts of the environment. This will be increasingly important in simulations of energy-transfer phenomena of protein−pigment complexes as occurring in natural photosynthetic systems.

Acknowledgment. J.N. is supported by a VIDI grant (700.59.422) of The Netherlands Organisation for Scientific Research (NWO) and acknowledges a computer time grant from the Stichting Nationale Computer Faciliteiten (NCF). C.C. acknowledges support from the Comissionat per a Universitats i Recerca of the Departament d'Innovació, Universitats i Empresa of the Generalitat de Catalunya, grant no. 2008BPB00108. A.M.-L. thanks support from the Spanish Ministerio de Ciencia e Innovación (Programa Nacional de Recursos Humanos del Plan Nacional I-D+I 2008−2011).

References

(1) Blankenship, R. E. *Molecular Mechanisms of Photosynthesis*; Blackwell Science: Oxford, 2002.

(2) Scholes, G. D. *Annu. Rev. Phys. Chem.* **2003**, *54*, 57–87.

(3) Förster, T. *Ann. Phys.* **1948**, *2*, 55.

(4) Förster, T. Delocalized Excitation and Excitation Transfer. In *Modern Quantum Chemistry. Part III: Action of Light and Organic Crystals*; Sinanoğlu, O., Ed.; Academic Press: New York, 1965; pp 93−137.

(5) Dexter, D. L. *J. Chem. Phys.* **1953**, *21*, 836–850.

(6) Harcourt, R. D.; Scholes, G. D.; Ghiggino, K. P. *J. Chem. Phys.* **1994**, *101*, 10521–10525.

(7) Krueger, B. P.; Scholes, G. D.; Fleming, G. R. *J. Phys. Chem. B* **1998**, *102*, 5378–5386.

(8) Damjanović, A.; Ritz, T.; Schulten, K. *Phys. Rev. E* **1999**, *59*, 3293–3311.

(9) Tretiak, S.; Middleton, C.; Chernyak, V.; Mukamel, S. *J. Phys. Chem. B* **2000**, *104*, 9540–9553.

(10) Tretiak, S.; Middleton, C.; Chernyak, V.; Mukamel, S. *J. Phys. Chem. B* **2000**, *104*, 4519–4528.

(11) Hsu, C.-P.; Fleming, G. R.; Head-Gordon, M.; Head-Gordon, T. *J. Chem. Phys.* **2001**, *114*, 3065–3072.

(12) Wong, K. F.; Bagchi, B.; Rossky, P. J. *J. Phys. Chem. A* **2004**, *108*, 5752–5763.

(13) Beenken, W. J. D.; Pullerits, T. *J. Chem. Phys.* **2004**, *120*, 2490–2495.

(14) Iozzi, M. F.; Mennucci, B.; Tomasi, J.; Cammi, R. *J. Chem. Phys.* **2004**, *120*, 7029–7040.

(15) Curutchet, C.; Mennucci, B. *J. Am. Chem. Soc.* **2005**, *127*, 16733–16744.

(16) Madjet, M. E.; Abdurahman, A.; Renger, T. *J. Phys. Chem. B* **2006**, *110*, 17268–17281.

(17) Neugebauer, J. *J. Phys. Chem. B* **2008**, *112*, 2207–2217.

(18) Muñoz-Losa, A.; Curutchet, C.; Fdez. Galván, I.; Mennucci, B. *J. Chem. Phys.* **2008**, *129*, 034104.

(19) Fink, R. F.; Pfister, J.; Zhao, H. M.; Engels, B. *Chem. Phys.* **2008**, *346*, 275–285.

(20) Hsu, C.-P. *Acc. Chem. Res.* **2009**, *42*, 509–518.

(21) Sagvolden, E.; Furche, F.; Köhn, A. *J. Chem. Theory Comput.* **2009**, *5*, 873–880.

(22) Neugebauer, J. *ChemPhysChem* **2009**, *10*, 3148–3173.

(23) Adolphs, J.; Renger, T. *Biophys. J.* **2006**, *91*, 2778–2797.

(24) Scholes, G. D.; Curutchet, C.; Mennucci, B.; Cammi, R.; Tomasi, J. *J. Phys. Chem. B* **2007**, *111*, 6978–6982.

(25) Russo, V.; Curutchet, C.; Mennucci, B. *J. Phys. Chem. B* **2007**, *111*, 853–863.

(26) Curutchet, C.; Scholes, G. D.; Mennucci, B.; Cammi, R. *J. Phys. Chem. B* **2007**, *111*, 13253–13265.

(27) Curutchet, C.; Muñoz-Losa, A.; Monti, S.; Kongsted, J.; Scholes, G. D.; Mennucci, B. *J. Chem. Theory Comput.* **2009**, *5*, 1838–1848.

(28) Tomasi, J.; Mennucci, B.; Cammi, R. *Chem. Rev.* **2005**, *105*, 2999–3094.

(29) Söderhjelm, P.; Husberg, C.; Strambi, A.; Olivucci, M.; Ryde, U. *J. Chem. Theory Comput.* **2009**, *5*, 649–658.

(30) He, Z.; Sundström, V.; Pullerits, T. *J. Phys. Chem. B* **2002**, *106*, 11606–11612.

(31) Timpmann, K.; Ellervee, A.; Pullerits, T.; Ruus, R.; Sundström, V.; Freiberg, A. *J. Phys. Chem. B* **2001**, *105*, 8436–8444.

(32) Neugebauer, J.; Louwerse, M. J.; Baerends, E. J.; Wesolowski, T. A. *J. Chem. Phys.* **2005**, *122*, 094115.

(33) Dreuw, A.; Weisman, J. L.; Head-Gordon, M. *J. Chem. Phys.* **2003**, *119*, 2943–2946.

(34) Tozer, D. *J. Chem. Phys.* **2003**, *119*, 12697–12699.

(35) Tawada, Y.; Tsuneda, T.; Yanagisawa, S.; Yanai, T.; Hirao, K. *J. Chem. Phys.* **2004**, *120*, 8425–8433.

(36) Gritsenko, O.; Baerends, E. J. *J. Chem. Phys.* **2004**, *121*, 655–660.

(37) Maitra, N. T. *J. Chem. Phys.* **2005**, *122*, 234104.

(38) Neugebauer, J.; Gritsenko, O.; Baerends, E. J. *J. Chem. Phys.* **2006**, *124*, 214102.

(39) Ziegler, T.; Seth, M.; Krykunov, M.; Autschbach, J. *J. Chem. Phys.* **2008**, *129*, 184114.

(40) Autschbach, J. *ChemPhysChem* **2009**, *10*, 1757–1760.

(41) Cortona, P. *Phys. Rev. B* **1991**, *44*, 8454–8458.

(42) Senatore, G.; Subbaswamy, K. R. *Phys. Rev. B* **1986**, *34*, 5754–5757.

(43) Wesolowski, T. A.; Warshel, A. *J. Phys. Chem.* **1993**, *97*, 8050.

(44) Wesolowski, T. A.; Weber, J. *Chem. Phys. Lett.* **1996**, *248*, 71–76.

(45) Iannuzzi, M.; Kirchner, B.; Hutter, J. *Chem. Phys. Lett.* **2006**, *421*, 16–20.

(46) Jacob, C. R.; Visscher, L. *J. Chem. Phys.* **2008**, *128*, 155102.

(47) *Amsterdam Density Functional program*; Theoretical Chemistry, Vrije Universiteit: Amsterdam. URL: http://www.scm-.com (access date: 01/17/2009).

(48) te Velde, G.; Bickelhaupt, F. M.; Baerends, E. J.; van Gisbergen, S. J. A.; Fonseca Guerra, C.; Snijders, J. G.; Ziegler, T. *J. Comput. Chem.* **2001**, *22*, 931–967.

(49) Casida, M. E.; Wesolowski, T. A. *Int. J. Quantum Chem.* **2004**, *96*, 577–588.

(50) Neugebauer, J. *J. Chem. Phys.* **2007**, *126*, 134116.

(51) Neugebauer, J. *J. Chem. Phys.* **2009**, *131*, 084104.

(52) Neugebauer, J. *Phys. Reports* **2010**, *489*, 1–87.

(53) Jacob, C. R.; Neugebauer, J.; Visscher, L. *J. Comput. Chem.* **2008**, *29*, 1011–1018.

(54) Wesolowski, T. A. *J. Am. Chem. Soc.* **2004**, *126*, 11444–11445.

(55) Davidson, E. R. *J. Comput. Phys.* **1975**, *17*, 87–94.

(56) Murray, C. W.; Racine, S. C.; Davidson, E. R. *J. Comput. Phys.* **1992**, *103*, 382–389.

(57) van Gisbergen, S. J. A.; Snijders, J. G.; Baerends, E. J. *Comput. Phys. Commun.* **1999**, *118*, 119–138.

(58) Wesolowski, T. A. *J. Chem. Phys.* **1997**, *106*, 8516–8526.

(59) Perdew, J. P. In *Electronic Structure of Solids*; Ziesche, P., Eschrig, H., Eds.; Akademie Verlag: Berlin, 1991; p 11.

(60) Lembarki, A.; Chermette, H. *Phys. Rev. A* **1994**, *50*, 5328.

(61) Frisch, M. J.; Trucks, G. W.; Schlegel, H. B.; Scuseria, G. E.; Robb, M. A.; Cheeseman, J. R.; Montgomery, J. A., Jr.; Vreven, T.; Kudin, K. N.; Burant, J. C.; Millam, J. M.; Iyengar, S. S.; Tomasi, J.; Barone, V.; Mennucci, B.; Cossi, M.; Scalmani, G.; Rega, N.; Petersson, G. A.; Nakatsuji, H.; Hada, M.; Ehara, M.; Toyota, K.; Fukuda, R.; Hasegawa, J.; Ishida, M.; Nakajima, T.; Honda, Y.; Kitao, O.; Nakai, H.; Klene, M.; Li, X.; Knox, J. E.; Hratchian, H. P.; Cross, J. B.; Bakken, V.; Adamo, C.; Jaramillo, J.; Gomperts, R.; Stratmann, R. E.; Yazyev, O.; Austin, A. J.; Cammi, R.; Pomelli, C.; Ochterski, J. W.; Ayala, P. Y.; Morokuma, K.; Voth, G. A.; Salvador, P.; Dannenberg, J. J.; Zakrzewski, V. G.; Dapprich, S.; Daniels, A. D.; Strain, M. C.; Farkas, O.; Malick, D. K.; Rabuck, A. D.; Raghavachari, K.; Foresman, J. B.; Ortiz, J. V.; Cui, Q.; Baboul, A. G.; Clifford, S.; Cioslowski, J.; Stefanov, B. B.; Liu, G.; Liashenko, A.; Piskorz, P.; Komaromi, I.; Martin, R. L.; Fox, D. J.; Keith, T.; Al-Laham, M. A.; Peng, C. Y.; Nanayakkara, A.; Challacombe, M.; Gill, P. M. W.; Johnson, B.; Chen, W.; Wong, M. W.; Gonzalez, C.; Pople, J. A. *Gaussian 03*, revision C.02; Gaussian, Inc.: Wallingford, CT, 2004.

(62) Dunning, T. H., Jr. *J. Chem. Phys.* **1989**, *90*, 1007–1023.

(63) Gagliardi, L.; Lindh, R.; Karlström, G. *J. Chem. Phys.* **2004**, *121*, 4494–4500.

(64) Humphrey, W.; Dalke, A.; Schulten, K. *J. Mol. Graphics* **1996**, *14.1*, 33–38.

(65) Kiewisch, K.; Eickerling, G.; Reiher, M.; Neugebauer, J. *J. Chem. Phys.* **2008**, *128*, 044114.

(66) Fux, S.; Kiewisch, K.; Jacob, C. R.; Neugebauer, J.; Reiher, M. *Chem. Phys. Lett.* **2008**, *461*, 353–359.

(67) Knox, R. S.; van Amerongen, H. *J. Phys. Chem. B* **2002**, *106*, 5289–5293.

CT100138K